Assessing Wrist Movement With Robotic Devices

Chad G. Rose, *Student Member, IEEE*, Evan Pezent, *Student Member, IEEE*, Claudia K. Kann, *Student Member, IEEE*, Ashish D. Deshpande, *Member, IEEE*, and Marcia K. O'Malley, *Senior Member, IEEE*

***Abstract*— Robotic devices have been proposed to meet the rising need for high intensity, long duration, and goal-oriented therapy required to regain motor function after neurological injury. Complementing this application, exoskeletons can augment traditional clinical assessments through precise, repeatable measurements of joint angles and movement quality. These measures assume that exoskeletons are making accurate joint measurements with a negligible effect on movement. For the coupled and coordinated joints of the wrist and hand, the validity of these two assumptions cannot be established by characterizing the device in isolation. To examine these assumptions, we conducted three user-in-the-loop experiments with able-bodied participants. First, we compared robotic measurements to an accepted modality to determine the validity of joint- and trajectory-level measurements. Then, we compared those movements to movements without the device to investigate the effects of device dynamic properties on wrist movement characteristics. Last, we investigated the effect of the device on coordination with a redundant, coordinated pointing task with the wrist and hand. For all experiments, smoothness characteristics were preserved in the robotic kinematic measurement and only marginally impacted by robot dynamics, validating the exoskeletons for use as assessment devices. Stemming from these results, we propose design guidelines for exoskeletal assessment devices.**

***Index Terms*— Robotic rehabilitation, exoskeleton, kinematic assessment, movement smoothness.**

I. Introduction

MORE than 90% of the seven million stroke survivors and half of the 282,000 individuals with spinal cord injury (SCI) in the United States require hand and wrist rehabilitation to regain the ability to perform activities of daily living (ADL) [1], [2]. For individuals with SCI, regaining upper extremity function is rated more desirable than regaining standing, bowel control, pain reduction, or sexual function [3]. In addition to the challenge of treating such a large population, the necessary rehabilitation regimens also require extensive (and often unavailable) resources to deliver high repetition, long duration, task-oriented movements aimed at recovering strength and coordination [4], [5]. To meet these labor, cost, and rising population needs, robotic devices have been proposed as tools for clinicians to provide accurate and repeatable high force movements and a means to record high-resolution, quantitative data needed to track therapeutic progress. These devices have been clinically verified for stroke and SCI rehabilitation [6]–[8]. For practical reasons, the same devices are often used for both delivering therapy and assessing outcomes [9].

Unlike functional assessments such as GRASSP [10] or Box and Blocks [11], robots afford clinicians high resolution measurements when assessing motor function. Several robotic measures have been proposed, examining aspects of motion in task and joint space. For example, Tyryshkin *et al*. [12] proposed tracking hand position during an object hitting task to create metrics which correlate with established measures in a post-stroke population. This precise Cartesian space trajectory tracking provides finer detail in assessing motor function than traditional methods, which rely on coarse measurements such as number of tasks completed within a specified time. Quantifying the intuitive notion of smoothness via precise robotic measures, particularly on the joint level via exoskeletons, will enable analyses not available to traditional clinical outcome measures or task-space metrics [13]–[15].

To examine these joint-level measures, it must be assumed that these devices, designed for training regimens, are 1) sufficient for inferring human joint angles and 2) do not alter the movements in a significant way. The first assumption may not be valid if there are misalignments between the robot and human joints or if the robotic kinematic structure oversimplifies the human joints (e.g., robotic pure rotational joint corresponding to human roti-translational joint). Apparent friction, inertia, and gravitational loads resulting in imperfect backdrivability, or insufficient dynamic transparency, would invalidate the second assumption. Typical experimental methods and

Manuscript received October 6, 2017; revised February 15, 2018; accepted June 27, 2018. Date of publication July 5, 2018; date of current version August 7, 2018. This work was supported in part by NSF under Grants NSF-CPS-1135916 and NSF-1250104 and NSTRF under Grant NNX13AM70H. *(Corresponding author: Chad G. Rose.)*

C. G. Rose, E. Pezent, and M. K. O'Malley are with the Mechanical Engineering Department, Rice University, Houston, TX 77005 USA (e-mail: cgr2@rice.edu).

C. K. Kann is with the Mechanical Engineering Department, Rice University, Houston, TX 77005 USA, and also with the Department of Mechanical and Civil Engineering, California Institute of Technology, Pasadena, CA 91125 USA.

A. D. Deshpande is with the Department of Mechanical Engineering, The University of Texas, Austin, TX 78712 USA.

Digital Object Identifier 10.1109/TNSRE.2018.2853143

metrics used to characterize robotic devices, such as system identification techniques for characterizing inertia, damping, and friction [16]–[18] are not sufficient to evaluate these assumptions since they do not evaluate the robot moving with a user's limb. It is critical to compare measurements from these experimental devices with an accepted, benchmark measurement modality that can track the human limb, such as electrogoniometry or motion capture [19]–[21]. This comparison is an especially critical and underreported validation for many exoskeleton designs [22], such as the IIT-Wrist [23] MIT-MANUS [14], InMotion3 [24], and the ARMin [25]. Further, this comparison will shed light on design guidelines to improve measurement capabilities of exoskeletons, and investigate the validity of simplified kinematic designs paired with passive degrees of freedom (DOF) to reduce overconstraint or hyperstaticity [17], [23], [26], [27]. Specifically, these tests will investigate the impact of movement with respect to the robot has on measurements, either along passive DOF or from the forces arising from hyperstaticity [28]. When testing the second assumption, examining the role that robotic dynamic properties play in influencing human movement will be particularly important [29]. It has been recognized that a robotic device's inherent dynamics can affect human movements, and researchers have proposed metrics to quantify their effect [30] and closed loop force control methods to mitigate these effects [31]. However, the impact of robot dynamics on measures of movement smoothness and coordination of the wrist have not been fully reported. Wrist pointing movements have been observed to be less smooth and more variable than pointing movements of elbow and shoulder [32]. Still, kinematic characterization of movement is an appealing method of assessment for rehabilitation applications since such movements can be measured non-invasively with the very robotic devices used to deliver treatment.

To this end, we designed three experiments to evaluate exoskeletons as wrist movement measurement devices using the exoskeletons and motion capture system introduced in Section II. Together, these three experiments form the set needed to validate exoskeletal measurements for assessment, and have protocols and measures well suited to replication on other devices. We examine the first assumption in isolation, by comparing robotic measurements to anatomic joint measurements (Section III). We then separate the effects of robot dynamics between joint-level effects (Section IV) and multi-articular coordination (Section V) to investigate the second assumption that robot dynamics have a negligible effect on movement. To conclude, design guidelines for exoskeletal measurement devices are discussed in detail in Section VI.

II. Measurement Modalities

In this section, we detail the measurement tools used to acquire and approximate human joint angles. In our experiments, we used several exoskeletons designed for the distal degrees of freedom of the upper limb, which constituted our *kinematic* measurement modality. These include the RiceWrist-S [17] (the wrist module of first version of READAPT [33]), the Maestro [34] (the READAPT hand module), and the OpenWrist [26], seen in Fig. 1. Pertinent information regarding these devices is summarized in this section. We also present an overview of the motion capture-based joint angle measurement, which constituted our *anatomic* measurement modality. Throughout this manuscript, we have represented anatomic and no-robot condition measurements in blue tones, with kinematic and robot condition measurements in red tones, and differences between them in purple tones.

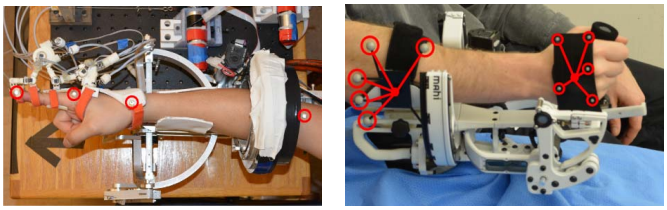

(a) (b)

Fig. 1. (a) READAPT [33] and (b) OpenWrist [26], the exoskeletons evaluated as a measurement devices via kinematic analysis. Marker placement highlighted in red, indicating point markers (circles) and rigid bodies used for anatomic joint measurement via passive optical motion capture.

A. Exoskeletons

The experimental wrist devices used to determine kinematic joint rotation are serial RRR exoskeletons with brushed DC motors and backlash-free capstan cable transmissions to apply torques to each DOF. All joint axes intersect perpendicularly at a single point, with a passive DOF at the handle to resolve kinematic overconstraint. These devices operate in a passive, unpowered backdrive mode when assessing movement, and rely on intrinsic device transparency [17] and optical encoders (resolutions $< 0.01°$) to approximate forearm pronation-supination (PS), wrist flexion-extension (FE), and wrist radial-ulnar deviation (RU). The hand module utilizes dynamic cancelation control to measure index, middle, and thumb metacarpalphalangeal (MCP) and proximal interphalangeal (PIP) joint angles. All devices meet or exceed the range of motion (ROM) requirements for ADL, the first requirement for assessment [17], [26], [34].

B. Motion Capture System

Optical motion tracking (NaturalPoint) is used to determine anatomic joint rotations. Six Optitrack Flex V100R2 100 FPS cameras track the positions of 5mm, (Fig. 1a), 3 mm, and 11 mm (Fig. 1b) markers to acquire relative anatomic joint angles during the pointing tasks. Markers are tracked as points in a plane (Fig. 1a) or as rigid bodies (Fig. 1b), which are then used to determine human joint angles. Joint angles are either approximated via a least-squares calibration [20], [35] (Section III and IV), or trigonometry [33] (Section V). The calibration takes the difference between the orientation of two rigid bodies, (in this case, the forearm and hand) in the world frame to estimate the axes of rotation based on single DOF calibration movements. Joint angles determined through trigonometry were approximated as co-planar, pure rotations, and were determined by tracking the position of

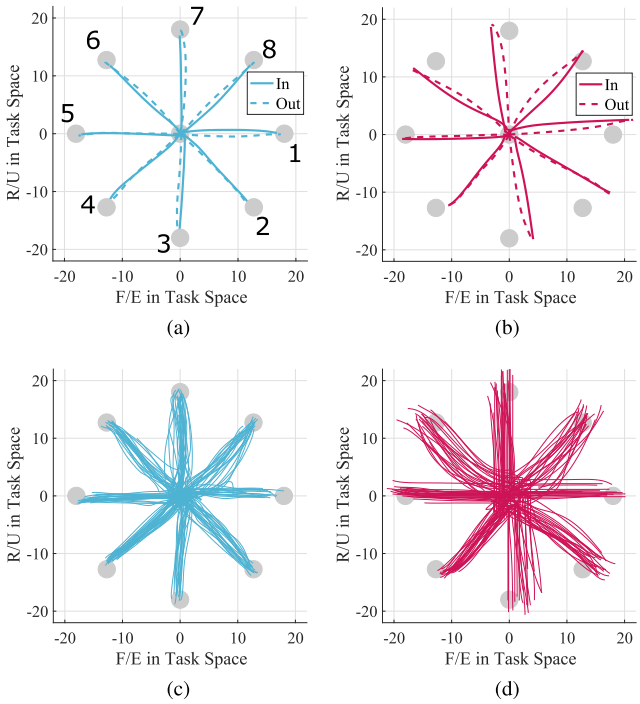

Fig. 2. Average (across all subjects) trajectories 2a, 2b and all inbound trials from one subject 2c, 2d, separated by measurement modality represent trends seen in the results. The differences between the trajectories are largely the result of the misalignment between the kinematic and anatomic joints, causing the kinematic trajectories to have additional curvature and seem to be rotated. Movement with respect to the robot, a likely source of error, is visible in the varied starting points in Fig. 2c and 2d. (a) Anatomic, task space. (b) Kinematic, task space. (c) Anatomic Inbound. (d) Kinematic Inbound.

markers placed at bony landmarks [19], [36], [37] circled in Fig. 1a. While there are limitations to placing markers on anatomical landmarks, this measurement process does improve repeatability within experiments, compared to methods that track a separate handle to make measurements [21].

III. Kinematic Vs. Anatomic Measurements

To investigate the assumption that measurements of robotic joint motion accurately reflect movements of the corresponding human joints, we recorded movements with both the human anatomic (motion capture) and robot kinematic (encoder) modalities while subjects completed a wrist pointing task. The goal of this experiment is to investigate and quantify the influence that both human-robot joint misalignment and movement with respect the robot have on kinematic measurements.

A. Experimental Methods

We designed a task requiring isolated and combined wrist FE and RU movements in the OpenWrist [26].

1) Task Description: The task consisted of pointing movements starting from a center, near neutral, position to one of eight outbound targets, displayed on a circle whose radius corresponded to a constant percentage (60%) of wrist ROM [38] as detailed in [35]. After reaching and remaining inside a target for one second, subjects would return to the center target, as seen in Fig. 2. After five practice pointing movements to each target, subjects performed fifteen reaching movements per target, in a pseudo-random order, for two speed conditions, with a visualization-suggested completion time (0.4 and 0.6 s). For all tasks, anatomic joint measurements were provided as visual feedback.

2) Subjects: Nine, able-bodied, right-hand dominant subjects (two female, seven male ages 20-28) completed the experiment in compliance with Rice University's Institutional Review Board, protocol number IRB-FY2016-96 (656800-4).

B. Data Analysis

Both kinematic and anatomic data were segmented with a 2% maximum velocity threshold to isolate individual reaching movements [14]. Anatomic measurements were filtered and differentiated with a third order Savitzky-Golay filter (21-sample, 200ms window) [39]. To investigate the degree of agreement between these measurement modalities, first, kinematic and anatomic joint measurements were compared in the joint space by calculating RMS error between individual trajectories. Then, two task-space measures of movement smoothness were computed: correlation to a minimum jerk speed profile (ρ) [15], and the spectral arc length (SAL) [13]. The first metric, ρ, compares a segmented velocity profile to a minimum jerk speed profile, which has been accepted as a benchmark for human pointing tasks [15], and ranges from not correlated (0) to perfectly correlated (1). SAL is the length of the Fourier magnitude spectrum of a segmented velocity profile, with unimpaired individuals' values in the -1 to -2 range, and impaired individuals' values upwards of -5. The default settings in the MATLAB function from Balasubramanian *et al.* [13] were used to compute SAL. A value (ρ or SAL) was considered an outlier if it fell three interquartile ranges below or above the 25th or 75th quartiles, respectively, and disqualified the corresponding trajectory from analysis (less than 1% of all trajectories were removed in this manner). Since our analysis examined the differences between anatomic and kinematic measurements, and not the preservation of properties dependent on speed or direction, all trajectories were analyzed together.

C. Experimental Results

Average trajectories across all subjects, and all inbound trajectories for a single subject are presented in the visualization space in Fig. 2. In addition to the characteristic curvatures and variability expected in wrist pointing tasks, a seeming 'rotation' of the FE and RU axes in Fig. 2b is apparent. This drove most of the error between joint-level measurements, caused by a difference in the orientations of the calibrated human joint axes and the orthogonal and intersecting joints of the robot.

The results suggest that unintended movement with respect to the robot could be the cause of the apparent spread of the starting positions of inbound trajectories (Fig. 2d) which reduce the repeatability of kinematic measures. Some inter-target variability, caused by the inter-subject variable differences between anatomic and kinematic axes also contributes to the variances in RMS in Fig. 3.

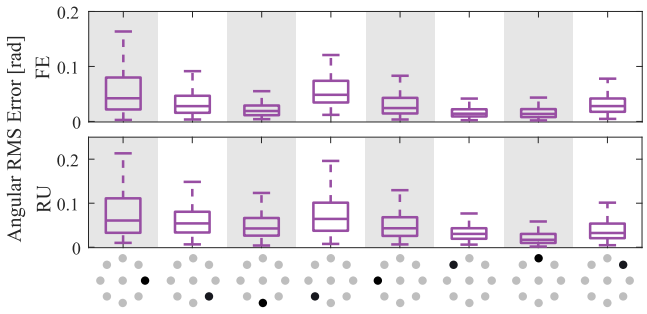

Fig. 3. RMS error values in radians separated by DOF and target, with single DOF targets in gray. Average errors across all targets were less than 0.062 radians. The variability is caused by range differences in the orientation of anatomic and kinematic joint axes between subjects.

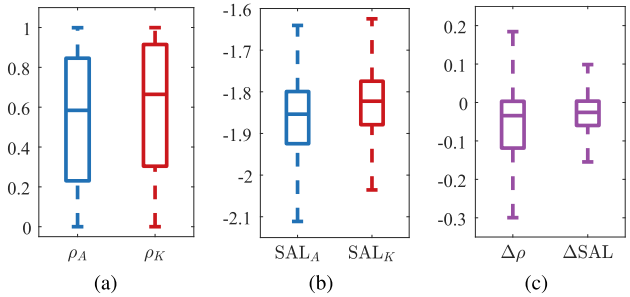

Fig. 4. Box plots for smoothness measures ρ (4a) and SAL (4b) across all subjects, with whiskers extending to 1.5 interquartile ranges past hinges. Human anatomic measures ($_A$) are presented on the left of each figure, with robot kinematic ($_K$) on the right. Shown in 4c, the difference between anatomic and kinematic measures is defined as $\Delta =$ *Anatomic-Kinematic*.

The RMS error between kinematic and anatomic measurements for each trajectory was calculated to quantify these observations (see Fig. 3). All targets had differences between the trajectories, stemming from the difference in anatomic and kinematic joint orientation which varied between subjects within the ranges previously reported [20]. The larger errors observed in some of the targets were likely caused by target-specific factors such as length of the path or ROM limits of the device, both of which impacted the fourth target's trajectories. Movements are consistently measured with both the anatomic and kinematic methods (average errors are less than 0.062 radians). The variance between these measurements is within ranges previously reported for goniometer-based measurements. Goniometry results in fairly high inter-observer variances, with standard deviations ranging between 3° and 10°, and intra-observer variance typically between 1° and 3° [40]. The variability in robotic wrist measurements is caused mainly by misalignment between the anatomic and kinematic joints, as well as limitations of the calibration process, which create an average wrist joint location. Our solution method, requiring simplification of the wrist joint to be two intersecting and orthogonal axes, with over-constraint resolved by a passive sliding DOF, detracts from the joint-level accuracy of kinematic measures. The difference between anatomic and kinematic joint orientations, and the variability of the anatomic joint axes that result from using robot kinematics to infer anatomic measurements of wrist position may limit the applicability of this approach for wrist movement assessment. Still, the observed degree of variability and RMS errors are no greater than that obtained from goniometry-based assessment of wrist movements. In fact, goniometers have been shown to have 'cross-talk' between FE and RU joints caused by complex wrist anatomy and simplifications made in goniometer design [41], the same challenges that we face in exoskeleton design for wrist assessment.

While the ability to use exoskeletal devices as goniometers for measuring ROM, most robotic metrics of motor function are based on a movement's tangential velocity in task space. This construction is particularly valuable for the wrist, where using the tangential velocity would reduce the effect of errors in joint axes estimation using robot encoder data.

TABLE I
DIFFERENCE VALUES BETWEEN MEASUREMENT MODALITIES (A-K)

	t-score	Confidence Interval	Correlation	Pooled σ
ρ	-3.73	(-0.094, -0.021)	0.94	0.044
SAL	-8.70	(-0.041,-0.023)	0.76	0.010

To compare the kinematic and anatomic measurements, a paired t-test was performed, with ρ and SAL values averaged across subjects and targets, shown in Table I. Even though there was a statistically significant difference in these measures, they remain highly correlated. Furthermore, the pooled standard deviations (σ) are approximately one order of magnitude smaller than the average standard deviations for a subject's movements (average standard deviation for ρ and SAL were 0.30 and 0.11, respectively), suggesting further that although these differences are statistically significant, they are well within the expected variability of human movement.

IV. Impact of Robot Dynamics on Wrist Kinematics

Next, to validate the exoskeletons as assessment tools, we investigated the role of robot dynamics on measurements. One intuitive way of performing these tasks is through comparisons between trajectories with and without the robotic assessment device. We hypothesized that the inertia and friction properties of the device would have a smoothing effect on the trajectories.

A. Experimental Methods

We compared data from the previous experiment to movements acquired from the same subjects using the protocol described in Section III-A without the OpenWrist exoskeleton.

B. Data Analysis

Joint measurements were segmented and the same outliers were removed as described in Section III-B. In addition to the movement smoothness metrics previously calculated (ρ and SAL), two wrist curvature metrics A_{sum} and A_{net} [21] were computed to examine the effect of robot dynamics on measured biomechanical properties. A_{sum} represents the total

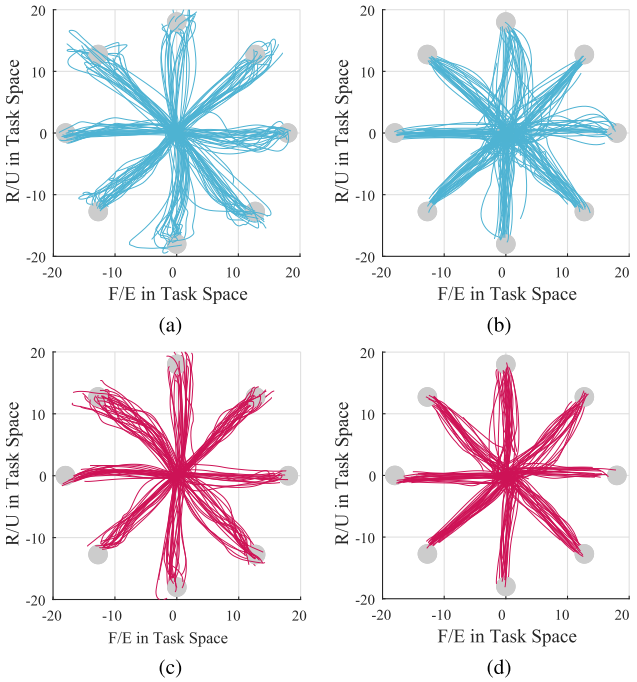

Fig. 5. All trajectories from one subject, in the visualization space, which suggest the robot may have a smoothing effect on wrist movements. (a) No Robot Outbound. (b) No Robot Inbound. (c) Robot Outbound. (d) Robot Inbound.

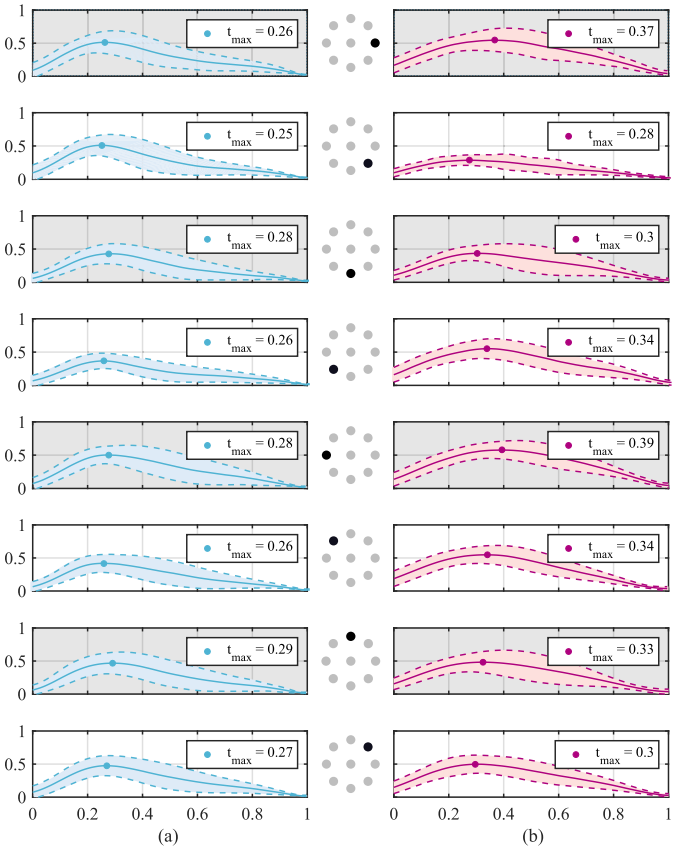

Fig. 6. Normalized velocity plots with average and one standard deviation bounds show that robot dynamics create a more qualitatively smooth and symmetric (less skew) velocity profile. Particularly, movement smoothness as capture by ρ values will be higher for the single DOF movements (gray background), with isolated FE (target 1 and 5) exhibiting the largest change. (a) No Robot. (b) Robot.

sum of the area between the trajectory and a straight line path, and A_{net} represents the difference between the area on the right and left of the straight line path ($\mathrm{R} - \mathrm{L} = A_{net}$).

We analyzed the effect of robot dynamics on each metric with a linear mixed-effects model, using the `lmer` [42] and `car` [43] packages in `R` [44]. Each metric was modeled as a function of condition (robot/no robot), target (1-8), direction (inbound/outbound), speed (fast/slow), as well as interactions between condition and the other three as fixed effects, with a random effect (intercept) of subject. This model assumes that there are fundamental between-subject differences, but the effect of condition, target, direction, speed, as well as the interaction between them is subject-independent.

C. Experimental Results

We observed differences in movements made with and without the OpenWrist. Fig. 5 presents all trajectories from a single representative subject, displaying a few of the key differences between the conditions. For example, the trajectories to and from Target 1, corresponding to an isolated wrist extension movement, are much straighter, and more tightly grouped for the movements made within the robot compared to those without the robot. This general trend persists for the remaining seven targets, but is less exaggerated for the multi-DOF targets.

The differences between single- and multi-DOF movements can be viewed in their velocity profiles, shown in Fig. 6. Single-DOF movements have a gray background, and combined FE/RU movements are in white. Single DOF movements' skewness is particularly of interest. Isolated FE movements appear to have the greatest change in skewness of any of the targets, and the isolated RU movements are the least changed, similar to results described in [29]. The timing of the multi-DOF movements' velocity peaks seems to be relatively unchanged when backdriving the robot, with an even distribution across the normalized time scale.

The impact of assessing with the robot is illustrated further in Fig. 7. The robot has a major impact on the smoothness correlation coefficient ρ. Movements made in the robot were considerably more correlated with the minimum jerk trajectory than those made in the no-robot condition. Two important quantifications of prior observations can be made. First, the qualitative observations about the skewness of isolated FE movements are supported by the largest mean values and increase over the no-robot condition. These targets correspond with movements which required the most motion on the second robot joint. Second, isolated RU movements are the least affected by the robot. Two conclusions could be drawn from these observations. First, the FE joint's inertia is approximately $10\times$ larger than the RU joint's [26]. The increased inertial load could act as a mechanical low-pass filter, having a smoothing effect on the movement profile. This would agree with observations of wrist movements in [45], where inertial loads tended to aid movements in following a minimum jerk trajectory. The second possibility is that friction in the RU joint, higher due to its complex cable routing,

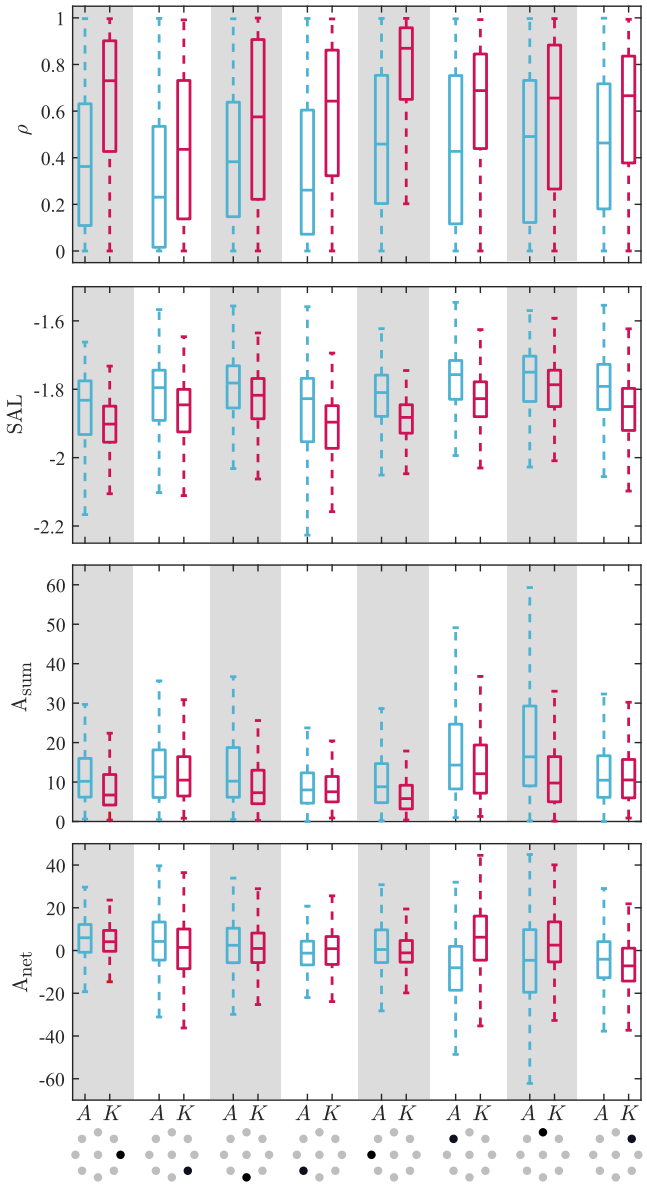

Fig. 7. Box plots of ρ, SAL, A_{sum}, and A_{net} values across all subjects and conditions, separated by target and measurement modality (anatomic on left, kinematic on right). Whiskers extend 1.5 times the interquartile range. Robot inertia and friction increased the ρ values. Unlike ρ, SAL decreased slightly, indicating that the robot only somewhat perturbed movements. Since trajectories with the robot were straighter, A_{sum} is lower, especially for single-DOF movements. The changes in A_{net} also seem to be DOF-dependent.

negatively impacts smoothness. This may explain why isolated RU targets do not experience the same increase in smoothness as isolated FE. Finally, the high degree of variability of ρ compared to SAL matches previously reported values [15], and deficiencies of the jerk-based measure [13].

The bar plots for SAL show that movements performed in robot were not very different from movements performed without the robot, and there is a decrease in the perceived smoothness of the trajectories. There is also much less variability in SAL compared to ρ. The values for SAL, around -1.9 for most targets, agree with values reported in [13] for healthy subjects. Since SAL can fall as low as -5 for stroke

TABLE II
RESULTS OF LINEAR MIXED-EFFECTS MODEL DETAILING EFFECT OF CONDITION, TARGET, DIRECTION, AND SPEED ON ρ, SAL, A_{sum}, AND A_{net}

		ρ	SAL	A_{sum}	A_{net}
Condition	NR	0.410*	-1.84*	14.24	-0.266
	R	0.598*	-1.88*	11.39	1.77
Target	Min	0.383*†	-1.93*	8.72*†	-5.35*†
	Max	0.618*†	-1.81*	13.91*†	6.02*†
Direction	In	0.490*	-1.85*	10.94*	-0.514
	Out	0.518*	-1.87*	14.69*	2.021
Speed	F	0.509	-1.85*	12.97	0.886
	S	0.499	-1.87*	12.67	0.621

TABLE III
EXAMINING EFFECT OF CONDITION SEPARATED BY TARGET TYPE

	FE Targets		RU Targets		Multi-DOF	
	NR	R	NR	R	NR	R
ρ	0.429	0.736	0.430	0.577	0.392	0.616
SAL	-1.86	-1.89	-1.81	-1.82	-1.83	-1.86
A_{sum}	11.22	4.00	17.91	5.91	13.78	6.41
A_{net}	3.44	1.11	-1.64	1.90	-1.78	0.243

subjects [13], it seems reasonable to conclude that the robot did not have a detrimental affect on SAL.

As seen in Fig. 5, movements within the robot were straighter, and therefore A_{sum} is lower, particularly for single-DOF (gray) targets. For multi-DOF (white) targets, A_{net} changed signs, and in general became larger in magnitude.

Results from the linear mixed-effects model are summarized in Table II where mean values of ρ, SAL, A_{sum}, and A_{net} (averaged across subject, target, direction, and speed as appropriate), with significant main effect of the category (far left column) indicated by *, and the presence of a significant interaction with condition indicated by †.

Specifically, there was a significant main effect of condition for ρ ($\chi^2(1) = 22.73$, $p < .001$) and SAL ($\chi^2(1) = 10.61$, $p = .001$). Although the change in SAL is significant, the difference between the means, shown in Table II, is very small. Similarly, the significant main effects for direction on ρ ($\chi^2(1) = 7.54$, $p < .001$), SAL ($\chi^2(1) = 4.44$, $p = .035$), and A_{sum} ($\chi^2(1) = 43.35$, $p < .001$) and the significant effect of speed on SAL ($\chi^2(1) = 5.97$, $p = .015$) also have small changes in mean. The effect of speed was the smallest out of all conditions. As expected, direction affected A_{sum} and A_{net}, but the variability of A_{net} values likely prevented the difference from being significant. There was a significant main effect of target for each metric (ρ: $\chi^2(7) = 41.11$, $p < .001$; SAL:$\chi^2(7) = 91.56$, $p < .001$; A_{sum}: $\chi^2(7) = 162.22$, $p < .001$; A_{net}:$\chi^2(7) = 89.14$, $p < .001$), which follows commentary that the pointing distance of a percentage of ROM made some targets more difficult than others [35].

To investigate the significant interaction between condition and target for ρ ($\chi^2(7) = 44.41$, $p < .001$) A_{sum} ($\chi^2(7) = 27.56$, $p < .001$) and A_{net} ($\chi^2(7) = 88.38$, $p < .001$), and further quantify the previous DOF-dependent observations, Table III reorganizes the information presented in Table II and regroups the mean values from the linear mixed-effects model

into average values for the single-DOF FE (Targets 1 and 5) and RU (Targets 3 and 7) targets as well as multi-DOF targets (Targets 2, 4, 6, and 8), as described in Fig. 2a. These values further support SAL as a valid robotic assessment metric, and underscore the DOF-dependent observations, namely that inertia contributes greatly to smoothness as quantified by ρ. Also, the difference between the isolated FE and RU movements further explains the interaction between condition and target, suggesting that, while the robot consistently changed the measures, FE inertia had a greater impact than RU friction. A_{sum} and A_{net} are the least changed for multi-DOF movements, suggesting that wrist biomechanical properties are best preserved when inertia and friction do not artificially constrain movement to one robot DOF.

V. Impact of Robot Dynamics on Coordinated Hand-Wrist Movements

The previous results suggest that robotic assessment can affect coordinated movement in different ways, with aspects of movement smoothness increasing (ρ), and aspects of movement quality decreasing (SAL). However, the near collocation and coupling of the RU and FE joints may not generalize to couplings between more disparate coordinated joints, such as the hand and wrist. In addition to the functional coordination required to perform ADL, the hand and wrist are also kinematically and dynamically linked due to tendon and muscle anatomy [46], which extends to biomechanical couplings which manifest themselves in finger and wrist position-dependent passive properties [47], [48]. Loss of coordinated joint control is a key disability to overcome in stroke and SCI rehabilitation, and one of the main therapeutic targets for Parkinson's disease [49]. Due to its importance in rehabilitation and the preceding results, the impact of robot dynamics on coordinated hand-wrist movements is our next focus.

A. Experimental Methods

To explore wrist and hand coordination, we designed a redundant, planar pointing task requiring movement of the MCP and wrist FE joints either unconstrained or in the first version of the READAPT [33]. The task's redundancy arises from the 1D manifold of satisfactory MCP and FE angle solutions. These solution configurations can be separated into in-phase (same direction) and out-of-phase (opposite directions) movements based on the relative motion of the finger and wrist joints, following [47].

1) Task Description: Subjects pointed to targets in one of two locations by flexing or extending the wrist and flexing or extending the MCP joint. This pointing movement could be achieved with a user-selected movement coordination between wrist and MCP (unconstrained, UC) with both joints forced to be flexed or both extended (in-phase, IP) or with one joint flexed and the other extended (out of phase, OP). All solution configurations and target locations are shown in Fig. 8, with the planar mapping between MCP and wrist FE and the visualization shown in Fig. 8a. Different solution configurations were achieved by making the position of the obstacles a function of the wrist and finger angles, reducing the solution manifold as shown in Fig. 8. The planar mapping of the joints was ensured by constraining subjects' forearms to a planar surface. Subjects received tasks grouped by their solution configuration, either unconstrained (Fig. 8a and 8d), in-phase (Fig. 8b and 8e), or out-of-phase (Fig. 8c and 8f).

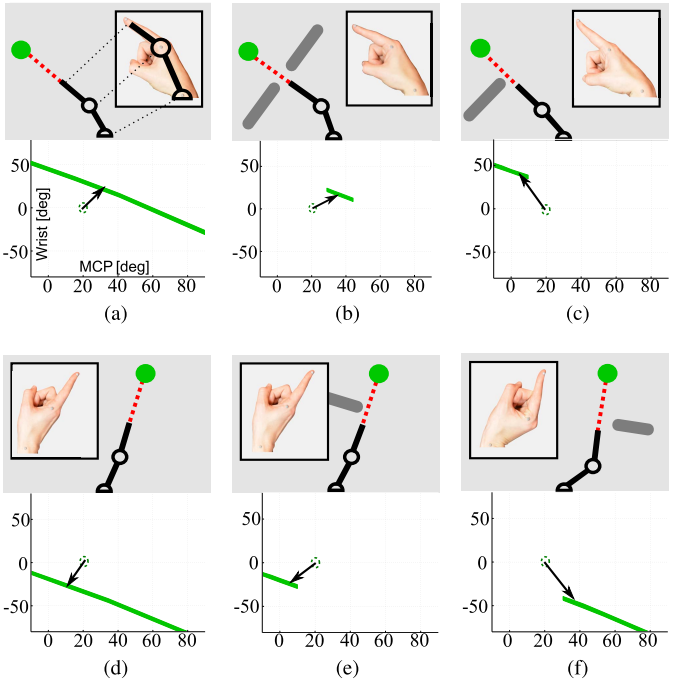

Fig. 8. Each subfigure shows one task, with the visualization and corresponding hand pose on top. The bottom figure is the solution manifold, in green, of joint angles that reach the target and avoid the obstacle, with MCP and wrist FE as the horizontal and vertical axes, respectively. (a) UC flexion. (b) IP flexion. (c) OP flexion. (d) UC extension. (e) IP extension. (f) OP extension.

The tasks were grouped by solution configuration, and subjects performed the unconstrained tasks first, then the constrained configurations, with breaks to prevent fatigue. Each task was initialized by requiring a movement to a neutral position before a pseudo random target (flexion or extension) would be presented, and each task ended once a subject had pointed at the target for one second. Subjects performed ten training movements for each target in each solution configuration, then fifty pseudorandomized tasks. Subjects then repeated this protocol while wearing the robot.

2) Subjects: Nine right hand dominant, able-bodied subjects (eight female, one male), ages 21-30 completed the study in compliance with Rice University's Institutional Review Board, protocol number IRB-FY2016-96 (656800-4).

B. Data Analysis

We characterized the interaction between the robot and natural movement with the time between joint velocity peaks, (inter-peak time) and the maximum deviation from a straight line in the joint space (straight line deviation). A coordinated movement should have simultaneous execution, resulting in low inter-peak times and straight line deviations. We hypothesized that the exoskeleton could distort synergistic

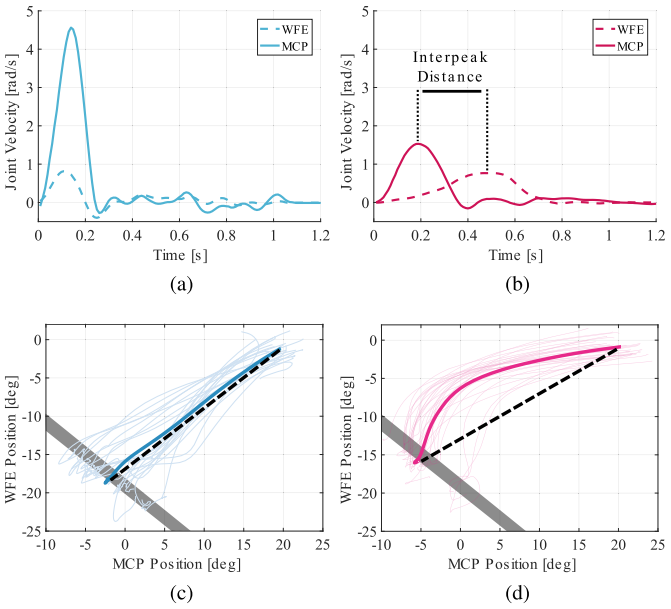

Fig. 9. Sample trajectories highlighting the discoordination characteristics. The example trajectory in 9a supports our hypothesis that natural movements have simultaneous velocity peaks, and discoordination manifest as time between finger and wrist velocity peak in the robot task (9b). The trajectories, when viewed in the joint-space (9c, 9d) also confirm hypotheses concerning straight line deviation. For these tasks, the solution manifold is in gray, average straight line path in dotted green, with individual and average trajectories in blue or red. The characteristic of discoordination is the movement along the axes (9d), instead of the simultaneous movement (9c). (a) NR Unconstrained Flexion. (b) R Unconstrained Flexion. (c) NR Unconstrained Extension. (d) R Unconstrained Extension.

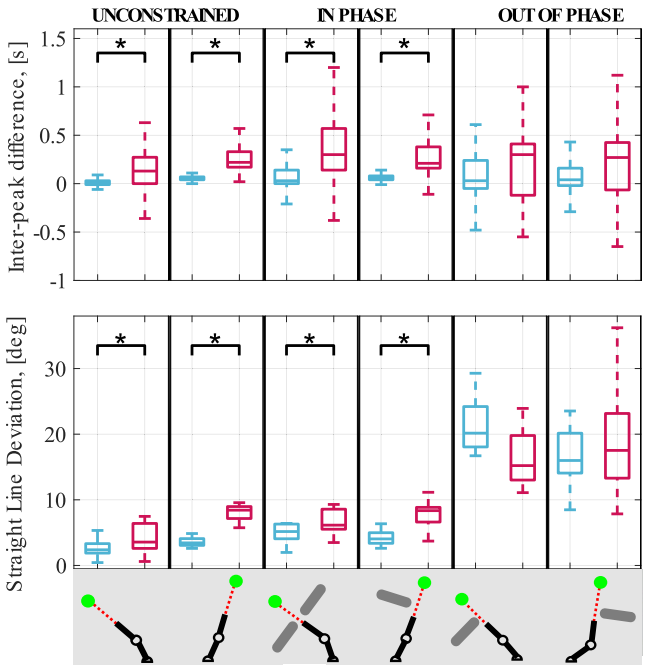

Fig. 10. Interpeak time (IPT, top) and Straight Line Deviation (SLD, bottom) results. Unconstrained and in-phase tasks were effected by the robot in a statistically significant way, likely due to the greater inertial and friction characteristics of the wrist exoskeleton. However, the difference was not significant for the unfamiliar out-of-phase movements, which may not possess the same strong coordination as the in-phase and unconstrained.

multi-DOF trajectories into sequential single-DOF movements.

Filtering and differentiation were accomplished via a third-order Savitzky-Golay filter with a 21-sample (200 ms) window. Inter-peak time was defined as $\Delta T = t_{p,w} - t_{p,MCP}$, where positive values indicate the MCP joint preceded the wrist. The maximum distance between the trajectory and a straight line path between the initial and final positions was defined as the straight line deviation. One measure was considered an outlier by falling outside of three interquartile ranges from the 25^{th} or 75^{th} percentile, and the corresponding trajectory was removed from analysis. Mean deviations of these metrics were analyzed through a factorial repeated ANOVA.

C. Experimental Results

The data presented in Fig. 9 suggests that wearing the robot resulted in the distortion of multi-DOF, coordinated trajectories into sequential, single-DOF movements, where the MCP joint precedes FE movement, resulting in higher values for both IPT and SLD. The unconstrained movements in Fig. 10 show that natural pointing involves simultaneous movement, as evidenced by the tightly grouped, small magnitudes for IPT and SLD. Second, this plot suggests that natural in-phase movements are similar to unconstrained movements, with similar values on both inter-peak time and straight line deviation. For both of these movement types, the interaction with the robot perturbed the coordination, increasing the magnitude and variability of both measures.

TABLE IV
EFFECT OF ROBOT ON INTER-PEAK TIME AND STRAIGHT LINE DEVIATION

	Inter-peak Time			Straight Line Deviation		
	F(1,8)	p	η_p^2	F(1,8)	p	η_p^2
UC	28.6	0.001	0.781	20.4	0.002	0.710
IP	36.7	<0.001	0.82	26.6	0.001	0.769
OP	3.6	0.095	0.31	2.1	0.185	0.208

There was an interaction between no-robot/robot and movement category for both interpeak time ($F(1.26, 10.05) = 5.4$, $p = 0.04$, $\eta_p^2 = .40$) and straight line deviation ($F(1.45, 11.6) = 17.35$, $p = 0.001$, $\eta_p^2 = .68$). Decomposing these interactions using simple main effects showed an effect for unconstrained and in-phase movements, but not for out-of-phase movements, as described in Table IV.

VI. Discussion

In this paper we present results from three experiments designed to investigate the implicit assumptions made when using exoskeletons for motor function assessment. These key assumptions are that 1) the kinematic measurements from the device correspond to anatomic joint measurements and 2) kinematic movement properties are preserved when using the robot as a measurement device.

The first experiment (Section III) examined robot kinematic and human anatomic joint measurements. Specifically, we

investigated the impact of robot joint orientation on inferences of human joint angle measurements. The trajectories suggest that simplifications in robot kinematic design decrease the accuracy of joint-level wrist measurement with the device but are comparable to accepted goniometric measurements. Broadly, while device inertia and friction helped 'smooth' trajectories, the soft connection between the robot and the human will always allow for some anatomic movement with respect to the robot, smoothing movement in a similar manner. Both of these negative effects should be taken into account, particularly when describing movement analyses. Furthermore, coupling between the wrist FE and RU joints suggests that analyses of movements about perpendicular flexion/extension and radial/ulnar deviation axes may obscure important coupled characteristics. It is the authors' opinion that analyses of isolated wrist DOFs are problematic regardless of measurement modality, which has been suggested previously [41]. Therefore, we recommend that coordinated FE and RU velocity profiles be analyzed together with intuitive metrics such as ρ (correlation to a minimum jerk trajectory) and SAL (length of Fourier magnitude spectrum). Furthermore, movements characteristics ρ and SAL are preserved in both methods of data collection (via robotic or via motion capture of anatomic joint measurements). We observed small effect sizes and high correlations between measurement modalities. Together, these findings suggest that robot kinematics reasonably replicate accepted goniometry and accurately capture movement characteristics of the wrist.

The second experiment examined the effect of the robot on natural movement. Analysis of movement smoothness metrics, ρ and SAL revealed two ways that movement was impacted by the human-robot interactions. Inertia and static friction in robot joints tend to increase ρ by reducing skewness of movements, and filtering corrective submovements, and this effect was greater for the joint with the greater inertia [29]. This observation, along with the changes measured by SAL, strongly suggests that robotic joints actuating each wrist DOF should ideally have small and matching dynamic properties. In this particular case, the RU robotic joint is only double the inertia of the hand [26], [50], and made only a small effect. These experiments further support the use of SAL for wrist movement smoothness measurement analysis, in that SAL is largely preserved when movements are measured via a robotic device compared to motion capture of anatomic movements.

The DOF-dependent results of A_{sum} and A_{net} also reveal guidelines for analysis and device design. The consistently lower A_{sum} values, along with some of the lower A_{net} values for single-DOF movements suggest that the inertia and static friction of the robot joint roughly perpendicular to the movement reduced the natural curvature of these movements, an effect not seen in the combined DOF movements. Several of the remaining A_{net} values changed sign, which could be the result of misalignment between the anatomic and kinematic joints. Since static friction and inertia can never be completely removed, ideal wrist assessment practices should engage multiple DOF to avoid this effect. Ideally, these multiple wrist DOF would have identical inertial properties which represent a small increase to the intrinsic inertia of the wrist. Similarly, the friction properties should be as small and isotropic as possible. In the case of the OpenWrist, the inertial and frictional properties are approaching satisfactory values, with most of the movement characteristics in Fig. 7 preserved, validating the use of this device for assessment. We expect that the relative importance of these design guidelines should decrease with lower device inertia and friction. While active compensation of device dynamics can be achieved with feed-forward torque control, this technique has been shown to have little impact on movement smoothness [29]. Devices that do not meet these design guidelines should only measure movements that engage multiple robotic DOF, to minimize the disturbance to smoothness characteristics. However, the impact of inertia is expected to be reduced with impaired users, since their relative velocities and coordination patterns are anticipated to be lower than those of able-bodied users.

The third experiment (Section V) examined the effect of the robot on coordinated movement. Since robot dynamics have an impact on the coupled dynamics of the wrist [38], [50], considering their impact on movements of non-collocated coupled joints, such as the hand and wrist, is important for rehabilitation of coordinated tasks. As expected, coordination, in the form of kinematic coupling of the velocity, was perturbed by the exoskeleton in a statistically significant way for natural movements. The inertia of the wrist module is likely the cause of this decoupling, with wrist FE inertia approximately five times larger than that of the wrist [50]. Commonplace movements may have more refined, and potentially sensitive, internal models used by the neuromuscular system [51], whereas the models for out of phase movements are less developed and potentially less likely to be disturbed. We expect individuals with significant motor impairment to not possess these highly refined and therefore sensitive models, and it is reasonable to expect their movements, like out of phase movements, to not be impacted by the robot.

In summary, we propose the following design guidelines for robotic devices intended as kinematic assessment tools:

1) Match device ROM to human capability [15], [17], [18].
2) Use high-resolution sensors [15], [17], [18]
3) Ensure anatomic and kinematic joint alignment via simplifications [17], [26] or individualized design [27]
4) Display low, isotropic inertia. Results suggest doubling intrinsic inertia is satisfactory for healthy individuals.
5) Minimize static friction in the device.
6) Engage multiple robotic DOF during assessment to reduce effects of friction on measurements.

Future work on robotic assessment of motor function should focus on the development and comparison of lightweight inertially isotropic devices and impedance-matched (as a proportion of joint inertia) anisotropic devices in experiments with healthy and impaired populations.

VII. Conclusion

To meet rising needs and leverage new assessment modalities, robots are being utilized in rehabilitation as therapeutic and assessment tools. Their measurement of joint and task space movement hinges on two assumptions. First, it is typically assumed that the human and robot joints are aligned,

and second, wearing the exoskeleton does not significantly impact movement. For multi-articular joints such as the wrist, validating these assumptions are not trivial. To investigate the validity of these assumptions, we conducted three experiments. First, we evaluated the accuracy of kinematic joint measurement compared to anatomic joint measurements. For the tested pointing task, the kinematic measures were comparable to accepted goniometry despite limitations caused by movement relative to the device and the variable (between subjects) and changing (within subjects) anatomic joint axes orientation. Kinematic measurements also preserved movement smoothness characteristics key to many robotic assessments. To investigated the second assumption, we conducted two experiments comparing movement with to movement without the robot. The second experiment identified effects of device inertia on wrist movement smoothness, and recommended the use of inertially isotropic wrist devices, with assessment not along robot joints, but rather of coordinated movements of both the human and robot joints. The last experiment examined the interaction between exoskeletons and hand-wrist motor coordination, and showed that familiar coordinations were perturbed for healthy individuals, but unfamiliar movements were not significantly impacted by the presence of a robotic assessment device. We hypothesize that these unfamiliar tasks constitute the bulk of movements made by individuals with neuromuscular motor impairment. Therefore, we conclude that the kinematic data from robotic wrist exoskeletons reliably represent human movement and preserves smoothness characteristics. Stemming from these results, we propose design guidelines for exoskeletons as measurement devices.

Acknowledgment

The authors would like to acknowledge Dr. Fabrizio Sergi for advice in the development of the experimental methods and Jennifer Sullivan for guidance on statistical analyses.

References

[1] D. Mozaffarian *et al.*, "Heart disease and stroke statistics—2016 update: A report from the American Heart Association," *Circulation*, vol. 138, no. 4, pp. e1–e324, 2016.

[2] National Spinal Cord Injury Statistical Center. (2017). *Spinal Cord Injury Facts and Figures at a Glance*. [Online]. Available: https://www.nscisc.uab.edu/Public/Facts%20and%20Figures%20-%202017.pdf

[3] G. J. Snoek, M. J. IJzerman, H. J. Hermens, D. Maxwell, and F. Biering-Sorensen, "Survey of the needs of patients with spinal cord injury: Impact and priority for improvement in hand function in tetraplegics," *Spinal Cord*, vol. 42, no. 9, pp. 526–532, 2004.

[4] P. R. Riener, T. Nef, and G. Colombo, "Robot-aided neurorehabilitation of the upper extremities," *Med. Biol. Eng. Comput.*, vol. 43, no. 1, pp. 2–10, Jan. 2005.

[5] C. Bütefisch, H. Hummelsheim, P. Denzler, and K.-H. Mauritz, "Repetitive training of isolated movements improves the outcome of motor rehabilitation of the centrally paretic hand," *J. Neurol. Sci.*, vol. 130, no. 1, pp. 59–68, 1995.

[6] D. J. Reinkensmeyer *et al.*, "Understanding and treating arm movement impairment after chronic brain injury: Progress with the ARM guide," *J. Rehabil. Res. Develop.*, vol. 37, no. 6, pp. 653–662, 2000.

[7] S. K. Charles, H. I. Krebs, B. T. Volpe, D. Lynch, and N. Hogan, "Wrist rehabilitation following stroke: Initial clinical results," in *Proc. IEEE Int. Conf. Rehabil. Robot. (ICORR)*, Jun. 2005, pp. 13–16.

[8] A. A. Blank, J. A. French, A. U. Pehlivan, and M. K. O'Malley, "Current trends in robot-assisted upper-limb stroke rehabilitation: Promoting patient engagement in therapy," *Current Phys. Med. Rehabil. Rep.*, vol. 2, no. 3, pp. 184–195, 2014.

[9] N. Yozbatiran *et al.*, "Robotic training and clinical assessment of upper extremity movements after spinal cord injury: A single case report," *J. Rehabil. Med.*, vol. 44, no. 2, pp. 186–188, 2012.

[10] S. Kalsi-Ryan, A. Curt, M. C. Verrier, and M. G. Fehlings, "Development of the Graded Redefined Assessment of Strength, Sensibility and Prehension (GRASSP): Reviewing measurement specific to the upper limb in tetraplegia," *J. Neurosurg., Spine*, vol. 17, pp. 65–76, Sep. 2012.

[11] V. Mathiowetz, G. Volland, N. Kashman, and K. Weber, "Adult norms for the box and block test of manual dexterity," *Amer. J. Occupat. Therapy*, vol. 39, pp. 386–391, Jun. 1985.

[12] K. Tyryshkin *et al.*, "A robotic object hitting task to quantify sensorimotor impairments in participants with stroke," *J. Neuroeng. Rehabil.*, vol. 11, p. 47, Apr. 2014.

[13] S. Balasubramanian, A. Melendez-Calderon, and E. Burdet, "A robust and sensitive metric for quantifying movement smoothness," *IEEE Trans. Biomed. Eng.*, vol. 59, no. 8, pp. 2126–2136, Aug. 2012.

[14] B. Rohrer *et al.*, "Movement smoothness changes during stroke recovery," *J. Neurosci.*, vol. 22, no. 18, pp. 8297–8304, Sep. 2002.

[15] O. Celik, M. K. O'Malley, C. Boake, H. S. Levin, N. Yozbatiran, and T. A. Reistetter, "Normalized movement quality measures for therapeutic robots strongly correlate with clinical motor impairment measures," *IEEE Trans. Neural Syst. Rehabil. Eng.*, vol. 18, no. 4, pp. 433–444, Aug. 2010.

[16] H. I. Krebs *et al.*, "Robot-aided neurorehabilitation: A robot for wrist rehabilitation," *IEEE Trans. Neural Syst. Rehabil. Eng.*, vol. 15, no. 3, pp. 327–335, Sep. 2007.

[17] A. U. Pehlivan, F. Sergi, A. Erwin, N. Yozbatiran, G. E. Francisco, and M. K. O'Malley, "Design and validation of the RiceWrist-S exoskeleton for robotic rehabilitation after incomplete spinal cord injury," *Robotica*, vol. 32, no. 8, pp. 1415–1431, 2014.

[18] J. A. French, C. G. Rose, and M. K. O'Malley, "System characterization of MAHI Exo-II: A robotic exoskeleton for upper extremity rehabilitation," in *Proc. ASME Dyn. Syst. Control Conf.*, 2014, p. V003T43A006.

[19] R. Schmidt, C. Disselhorst-Klug, J. Silny, and G. Rau, "A marker-based measurement procedure for unconstrained wrist and elbow motions," *J. Biomech.*, vol. 32, no. 6, pp. 615–621, 1999.

[20] E. V. Biryukova, A. Roby-Brami, A. A. Frolov, and M. Mokhtari, "Kinematics of human arm reconstructed from spatial tracking system recordings," *J. Biomech.*, vol. 33, no. 8, pp. 985–995, 2000.

[21] S. K. Charles and N. Hogan, "The curvature and variability of wrist and arm movements," *Exp. Brain Res.*, vol. 203, no. 1, pp. 63–73, 2010.

[22] N. Nordin, S. Q. Xie, and B. Wünsche, "Assessment of movement quality in robot-assisted upper limb rehabilitation after stroke: A review," *J. Neuroeng. Rehabil.*, vol. 11, no. 1, p. 137, 2014.

[23] L. Masia, M. Casadio, P. Giannoni, G. Sandini, and P. Morasso, "Performance adaptive training control strategy for recovering wrist movements in stroke patients: A preliminary, feasibility study," *J. Neuroeng. Rehabil.*, vol. 6, no. 1, p. 44, 2009.

[24] L. Vaisman, L. Dipietro, and H. I. Krebs, "A comparative analysis of speed profile models for wrist pointing movements," *IEEE Trans. Neural Syst. Rehabil. Eng.*, vol. 21, no. 5, pp. 756–766, Sep. 2013.

[25] T. Nef, M. Mihelj, G. Kiefer, C. Perndl, R. Müller, and R. Riener, "ARMin-Exoskeleton for arm therapy in stroke patients," in *Proc. IEEE Int. Conf. Rehabil. Robot. (ICORR)*, Jun. 2007, pp. 68–74.

[26] E. Pezent, C. G. Rose, A. D. Deshpande, and M. K. O'Malley, "Design and characterization of the openwrist: A robotic wrist exoskeleton for coordinated hand-wrist rehabilitation," in *Proc. IEEE Int. Conf. Rehabil. Robot. (ICORR)*, Jul. 2017, pp. 720–725.

[27] M. Esmaeili, N. Jarrassé, W. Dailey, E. Burdet, and D. Campolo, "Hyperstaticity for ergonomie design of a wrist exoskeleton," in *Proc. IEEE Int. Conf. Rehabil. Robot. (ICORR)*, Jun. 2013, pp. 1–6.

[28] N. Jarrasse and G. Morel, "Connecting a human limb to an exoskeleton," *IEEE Trans. Robot.*, vol. 28, no. 3, pp. 697–709, Jun. 2012.

[29] A. Erwin, E. Pezent, J. Bradley, and M. K. O'Malley, "The effect of robot dynamics on smoothness during wrist pointing," in *Proc. IEEE Int. Conf. Rehabil. Robot. (ICORR)*, Jul. 2017, pp. 597–602.

[30] D. Campolo, D. Accoto, D. Formica, and E. Guglielmelli, "Intrinsic constraints of neural origin: Assessment and application to rehabilitation robotics," *IEEE Trans. Robot.*, vol. 25, no. 3, pp. 492–501, Jun. 2009.

[31] N. L. Tagliamonte, M. Scorcia, D. Formica, D. Campolo, and E. Guglielmelli, "Effects of impedance reduction of a robot for wrist rehabilitation on human motor strategies in healthy subjects during pointing tasks," *Adv. Robot.*, vol. 25, no. 5, pp. 537–562, 2011.

[32] L. H. Salmond and S. K. Charles, "Why are wrist rotations considerably less smooth than reaching movements?" in *Proc. 36th Annu. Meeting Amer. Soc. Biomech.*, 2012, pp. 1–2.

[33] C. G. Rose, F. Sergi, Y. Yun, K. Madden, A. D. Deshpande, and M. K. O'Malley, "Characterization of a hand-wrist exoskeleton, READAPT, via kinematic analysis of redundant pointing tasks," in *Proc. IEEE Int. Conf. Rehabil. Robot. (ICORR)*, Aug. 2015, pp. 205–210.

[34] P. Agarwal, J. Fox, Y. Yun, M. K. O'Malley, and A. D. Deshpande, "An index finger exoskeleton with series elastic actuation for rehabilitation: Design, control and performance characterization," *Int. J. Robot. Res.*, vol. 34, no. 14, pp. 1747–1772, 2015.

[35] C. G. Rose, C. K. Kann, A. D. Deshpande, and M. K. O'Malley, "Estimating anatomical wrist joint motion with a robotic exoskeleton," in *Proc. IEEE Int. Conf. Rehabil. Robot. (ICORR)*, Jul. 2017, pp. 1437–1442.

[36] N. A. Baker, R. Cham, E. H. Cidboy, J. Cook, and M. S. Redfern, "Kinematics of the fingers and hands during computer keyboard use," *Clin. Biomech.*, vol. 22, no. 1, pp. 34–43, 2007.

[37] P. Braido and X. Zhang, "Quantitative analysis of finger motion coordination in hand manipulative and gestic acts," *Hum. Movement Sci.*, vol. 22, no. 6, pp. 661–678, 2004.

[38] J. J. Crisco, W. M. Heard, R. R. Rich, D. J. Paller, and S. W. Wolfe, "The mechanical axes of the wrist are oriented obliquely to the anatomical axes," *J. Bone Joint Surg. Amer.*, vol. 93, no. 2, pp. 169–177, 2011.

[39] A. Savitzky and M. J. E. Golay, "Smoothing and differentiation of data by simplified least squares procedures," *Anal. Chem.*, vol. 36, no. 8, pp. 1627–1639, 1964.

[40] J. Hogeweg, M. Langereis, A. Bernards, J. Faber, and P. J. M. Helders, "Goniometry-variability in the clinical practice of a conventional goniometer in healthy subjects," *Eur. J. Phys. Med. Rehabil.*, vol. 4, no. 1, pp. 2–7, 1994.

[41] P. Jonsson and P. W. Johnson, "Comparison of measurement accuracy between two types of wrist goniometer systems," *Appl. Ergonom.*, vol. 32, no. 6, pp. 599–607, 2001.

[42] D. Bates, M. Maechler, B. Bolker, and S. Walker, "Lme4: Linear mixed-effects models using Eigen and S4," *R Package Version*, vol. 1, no. 7, pp. 1–23, 2014. [Online]. Available: https://github.com/lme4/lme4/

[43] J. Fox *et al.* (2017). *Package 'Car'*. [Online]. Available: https://cran.r-project.org/web/packages/car/index.html

[44] *The R Project for Statistical Computing*. Accessed: Jan. 12, 2018. [Online]. Available: https://www.r-project.org/

[45] R. Stein, F. Cody, and C. Capaday, "The trajectory of human wrist movements," *J. Neurophysiol.*, vol. 59, no. 6, pp. 1814–1830, 1988.

[46] Z.-M. Li, "The influence of wrist position on individual finger forces during forceful grip," *J. Hand Surg.*, vol. 27, no. 5, pp. 886–896, 2002.

[47] A. D. Deshpande, N. Gialias, and Y. Matsuoka, "Contributions of intrinsic visco-elastic torques during planar index finger and wrist movements," *IEEE Trans. Biomed. Eng.*, vol. 59, no. 2, pp. 586–594, Feb. 2012.

[48] J. S. Knutson, K. L. Kilgore, J. M. Mansour, and P. E. Crago, "Intrinsic and extrinsic contributions to the passive moment at the metacarpophalangeal joint," *J. Biomech.*, vol. 33, no. 12, pp. 1675–1681, 2000.

[49] N. Dounskaia, A. W. Van Gemmert, B. C. Leis, and G. E. Stelmach, "Biased wrist and finger coordination in Parkinsonian patients during performance of graphical tasks," *Neuropsychologia*, vol. 47, no. 12, pp. 2504–2514, 2009.

[50] S. K. Charles and N. Hogan, "Dynamics of wrist rotations," *J. Biomech.*, vol. 44, no. 4, pp. 614–621, 2011.

[51] D. M. Wolpert, Z. Ghahramani, and M. I. Jordan, "An internal model for sensorimotor integration," *Science*, vol. 269, no. 5232, pp. 1880–1882, 1995.